Experimental Research on the Failure Mechanism of Foam Concrete with C-Channel Embedment

Dianzhong Liu[1a], Fayu Wang[1*], Feng Fu[2b] and He Wang[3c]

[1] School of Civil Engineering, Jilin Jianzhu University, No.5088 Xincheng Avenue, Jingyue Economic Development Zone, Changchun, Jilin, CN 130118, People's Republic of China
[2] School of Mathematics, Computer Science & Engineering, Department of Civil Engineering, City, University of London, Northampton Square, London, EC1V 0HB, United Kingdom
[3] Faculty of Environmental Engineering, The University of Kitakyushu, 1-1 Hibikino, Wakamatsu-ku, Kitakyushu, Fukuoka, JP 808-0135, Japan

(Received keep as blank, Revised keep as blank, Accepted keep as blank)

Abstract. An experimental investigation is carried out on the failure mechanism of foam concrete with cold formed steel double C-Channels embedment. The foam concrete is made of cement and fly ash with a compressive strength between 9 and 24 MPa with different densities. Forty-eight tests have been carried out in four groups of specimens with various embedment depths of the steel in the concrete. Four modes of failure are observed, which include the independent failure of the C-Channels with and without a concrete block inside the channel as well as the combined failure of the two channels, and the failure of the extrusion block. A theoretical model has been developed to understand the failure process. The peak compressive force applied onto the C-Channels that causes failure is calculated. It is concluded that the failure involves independent slippage between two C-Channels, and the steel and the foam concrete blocks inside the C-Channels. A method to calculate the peak force is also developed based on the test results. The calculations also show that the shear strength of the foam concrete is about 8% of the compressive strength with α coefficient of 0.4 between the steel and concrete.

Keywords: bond-slip; C-Channel; cold formed steel; foam concrete; fly ash

1. Introduction

The foam concrete also known as cellular lightweight concrete or reduced density concrete is made of cement and fly ash with a compressive strength between 9 and 24 MPa with different densities. With a minimum of 20% (per volume) foam entrained into the plastic mortar. The density of foam concrete usually varies from 400 kg/m³ to 1600 kg/m³. The density is normally controlled by substituting fully or partially of the fine aggregate with foam. Foam concrete has been widely used for non-structural members in buildings, such as lightweight sound barriers, partition walls, as well as infill for masonry walls. it has good thermal insulation and fire resistance. Although foam concrete has been primarily used for non-structural members, there is an increasing trend for its use in structural support (Mohamad et al., 2014). The compression and flexural behaviour of foam concrete have been studied. Due to its inherent low density and low strength, foam concrete is often used with steel reinforcements or composites steel (Flores-Johnson and Li, 2012; Ikponmwosa et al., 2014).

Different way of strengthening foam concrete have been examined by various researchers. For instance, Wan Ibrahim et al. (2014) indicated that foam concrete is brittle and consequently carried out investigations to determine whether the addition of polyolefin fibres with a low volume fraction has any influence on the compressive and flexural strengths. They found that the properties of foam concrete are only marginally improved with the addition of polyolefin fibres. Nambiar and Ramamurthy (2008) studied the effects of the mixture composition on foam concrete and found that foam concrete is affected by the base mix consistency and the volume of the foam that is added into the other ingredients in the mixture. Mydin and Wang (2011) studied the properties of foamed concrete at higher temperatures and demonstrated through experimental work that temperatures higher than 90°C cause loss of stiffness in foam concrete with the expansion and evaporation of water from its pores, which results in micro cracking. It was also found that the density does not make any difference after 90°C. Lim et al. (2014) examined foam concrete with the addition of different amounts of sand and found that finer sand means a reduction in the quality of the foam concrete and 0.6 mm of sand optimizes the compressive and flexural properties. Yue and Bing (2015) used magnesia phosphate cement in lieu of Portland cement and produced lightweight foam concrete that has a strength of 1 to 2.8 MPa with a dry density that ranges from 210 to 380 kg/m³.

*Corresponding author, M.Sc. Research Assistant
E-mail: Fayu_Wang@outlook.com
[a] Ph.D. Professor, Dean
E-mail: dz105@163.com
[b] Ph.D. Lecturer
E-mail: cenffu@yahoo.co.uk
[c] Ph.D. Student
E-mail: y7dbb001@eng.kitakyu-u.ac.jp

However, when using steel embedment as a means of reinforcement to provide tensile, bending and compression resistance, the mechanical characteristics is found to be greatly improved (Heath, 2014), Warren G. E. (1969) Therefore, in this paper, the compressive load on an embedded double C-Channel has been experimentally studied and theoretically analysed. The objective of the work is to understand the bond-slip characteristics between steel and foam concrete. The failure mechanism of the steel-foam concrete is also investigated.

In studying the bond-slip characteristics between steel and foam concrete, Ramezani et al. (2013) carried out pull-out testing of galvanized steel strips in foam concrete. The bond-stress versus slip displacement showed a typical hardening and softening behaviours. In order to improve the anchorage of the steel strips, holes were punched into the steel. The pull-out resistance was found to be directly proportional to the area of the holes which represents more bonding between the steel and the concrete. However, their analysis showed that the steel strip experiences non-uniform straining which results in a larger displacement at the peak force when the bonding increases (by increasing the diameter and circumference of the holes).

Mohamad et al. (2014) performed laboratory tests on a precast lightweight foam concrete sandwich panel with double shear truss connectors as the structural member. The panel was simply supported and subjected to flexure bending. Only concrete density of 1800 kg/m^3 was taken into consideration. They observed that shear cracks develop in the foam concrete from the bottom of the panel.

Flores-Johnson and Li (2012) conducted experiments on plain and fibre reinforced foam concrete with corrugated steel panels. For a foam concrete density of 1200 kg/m^3, the uniaxial compressive strength of the concrete was measured to be about 5 MPa with a uniaxial compression elastic modulus of about 1 GPa. The fibre reinforced foam concrete had almost twice the uniaxial compressive strength, but a slight increase in the elastic modulus by about 20%. A typical stress-strain plot showed a peak compression followed by a rapid decrease in the resistance to a residual value. The residual value refers to the resistance of the material after reaching the peak value. The residual value was zero in some cases.

Ikponmwosa et al. (2014) conducted flexure tests on steel reinforced foam concrete. They found that the shear strength developed in the beam lies between 13% and 20% of the compressive strength of the foam concrete. However, Thakrele (2014) reported that the shear strength lies between 6% and 10% of the compressive strength of foam concrete. The compressive strength varied from 8 to 13 MPa for a foam concrete density range of approximately 1700 to 1900 kg/m^3. Hilal et al. (2015) studied the enhancement of the properties of foam concrete with silica fume and fly ash additives. When the density of the concrete varied from 1300 to 1900 kg/m^3, the compressive strength varied from 1.5 to over 5 MPa. Of course, the strength, both shear and compression depends on the density and composition of the foam concrete.

Tan et al. (2015) experimentally explored the compressive strength of foam concrete with densities of 1500 ± 50 kg/m^3 and used sand as the filler. They found that the compressive strength of foam concrete ranges from 6.5 to 9.4 MPa, and when the steel strips have holes, there is better pull out strength with the highest strength of 1.03 MPa.

From above literature review, though some research on the experimental tests of foam concrete have been conducted, little research for foam concrete with steel embedment has been made in the past, therefore the research on the foam concrete using steel embedment's was carried by the authors and the results is shown in this paper.

In the research presented in this paper, the density of the foam concrete varies from 800 to 1600 kg/m^3 which provide a good range of compressive and shear strengths. Laboratory tests have been carried out on foam concrete with C-Channel steel to study the bonding and interface characteristics of steel and concrete. All the tests are carried out in compression.

2. Test set up

A series of experiments were carried out in Jilin Jianzhu University to determine the failure mechanism of cold formed steel C-Channels embedded foam concrete. The dimensions of the concrete specimen and the C-Channels are shown in Figure 1A. As it shown in Figure 1B, vertical compressive forces are applied onto the C-Channels. The foam concrete specimen is supported at its base. The thickness of channels is 3 mm, with a length and width of 120 x 50 mm respectively. The embedment depth of the C-Channel in the foam concrete varied, depending on the size of the foam concrete block. The concrete block has a rectangular cross section of 440 x 360 mm and the embedment depth varies from 100 to 400 mm. In order to study the stress transfer from the channel to the foam concrete, four groups of specimens were tested. Groups A, B, C, and D have a specimen depth of 100, 200, 300 and 400 mm respectively (see Figure 2). Four different densities were studied in each group. The specimens had a density of 800, 1000, 1200 and 1600 kg/m^3 respectively. As it shown in Table 1, for each density of the foam concrete, three tests were carried out; to ensure the reproducibility of the results. Increases in density result in high compressive and shear strength as well as an increase in the modulus of the material.

Table 1 Configurations of Test Specimens

Group	Specimen Number	Depth (mm)	Foam Density (kg/m^3)	Stirrup Configuration	Stirrup Percentage
A	A1-A3	100	800	ϕ6@60[a]	0.55%
	A4-A6	100	1000	ϕ6@60	0.55%
	A7-A9	100	1200	ϕ6@60	0.55%
	A10-A12	100	1600	ϕ6@60	0.55%
B	B1-B3	200	800	ϕ6@80[b]	0.41%
	B4-B6	200	1000	ϕ6@80	0.41%
	B7-B9	200	1200	ϕ6@80	0.41%
	B10-B12	200	1600	ϕ6@80	0.41%
C	C1-C3	300	800	ϕ6@85[c]	0.39%
	C4-C6	300	1000	ϕ6@85	0.39%
	C7-C9	300	1200	ϕ6@85	0.39%

	C10-C12	300	1600	ϕ6@85	0.39%
D	D1-D3	400	800	ϕ6@90[d]	0.36%
	D4-D6	400	1000	ϕ6@90	0.36%
	D7-D9	400	1200	ϕ6@90	0.36%
	D10-D12	400	1600	ϕ6@90	0.36%

Note: Stirrup has 20 mm concrete cover.
[a] Denotes grade II bar, with diameter of 6 mm, and spacing of 60 mm.
[b] Denotes grade II bar, with diameter of 6 mm, and spacing of 80 mm.
[c] Denotes grade II bar, with diameter of 6 mm, and spacing of 85 mm.
[d] Denotes grade II bar, with diameter of 6 mm, and spacing of 90 mm.

2.1 Test arrangement

The reinforcement used in the foam concrete blocks are 6 mm diameter rebars with two to five stirrups, see Figure 2. The stirrups have a 20-mm concrete cover. The stirrups provide lateral support and confinement of the foam concrete blocks when they are subjected to vertical shear through the steel channels, thus minimizing the splitting failure of the concrete blocks.

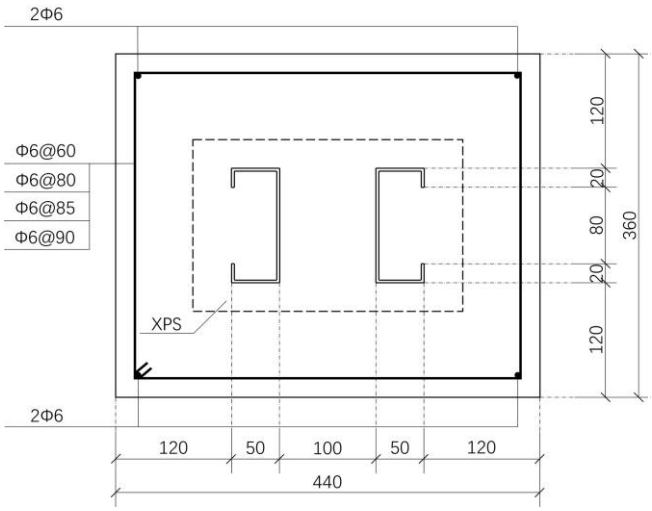

(a) Plan view of foam concrete specimens (XPS – extruded polystyrene to provide extrusion cavity, all dimensions in mm)

(b) Test Rigs

(c) Foam concrete specimens

Figs. 1 Foam concrete specimens and test arrangement

As it shown in Figure 1(c), the vertical compressive forces were loaded directly on the steel channels. In order to investigate longitudinal shear stress and slips between the steel channels and foam concrete, an extrusion void space was created at the bottom of the specimen by using polystyrene when the concrete was poured, see Figure 2 and 3. The extrusion space at the bottom of the specimen is 280 x 180 x 10 mm in size, thus allowing a maximum of 10 mm for the vertical displacement of the steel channel. A panel saw was used to cut the wood for the template which formed the mould for the foam concrete assembly, and double sided adhesive tape was used to hold tailored extrusion plates onto the bottom of the mould. Since the foam concrete has a low density, there is a good possibility that the foam bubbles could easily burst and evaporation would take place, thus resulting in higher volume shrinkage during curing. Therefore, the depth of the mould was slightly greater than the height specified in the design of the concrete specimen used for testing. The coupon test for the C channels and foam concrete cubes were also conducted in the same time to monitoring the strength of the C channels and foam concretes.

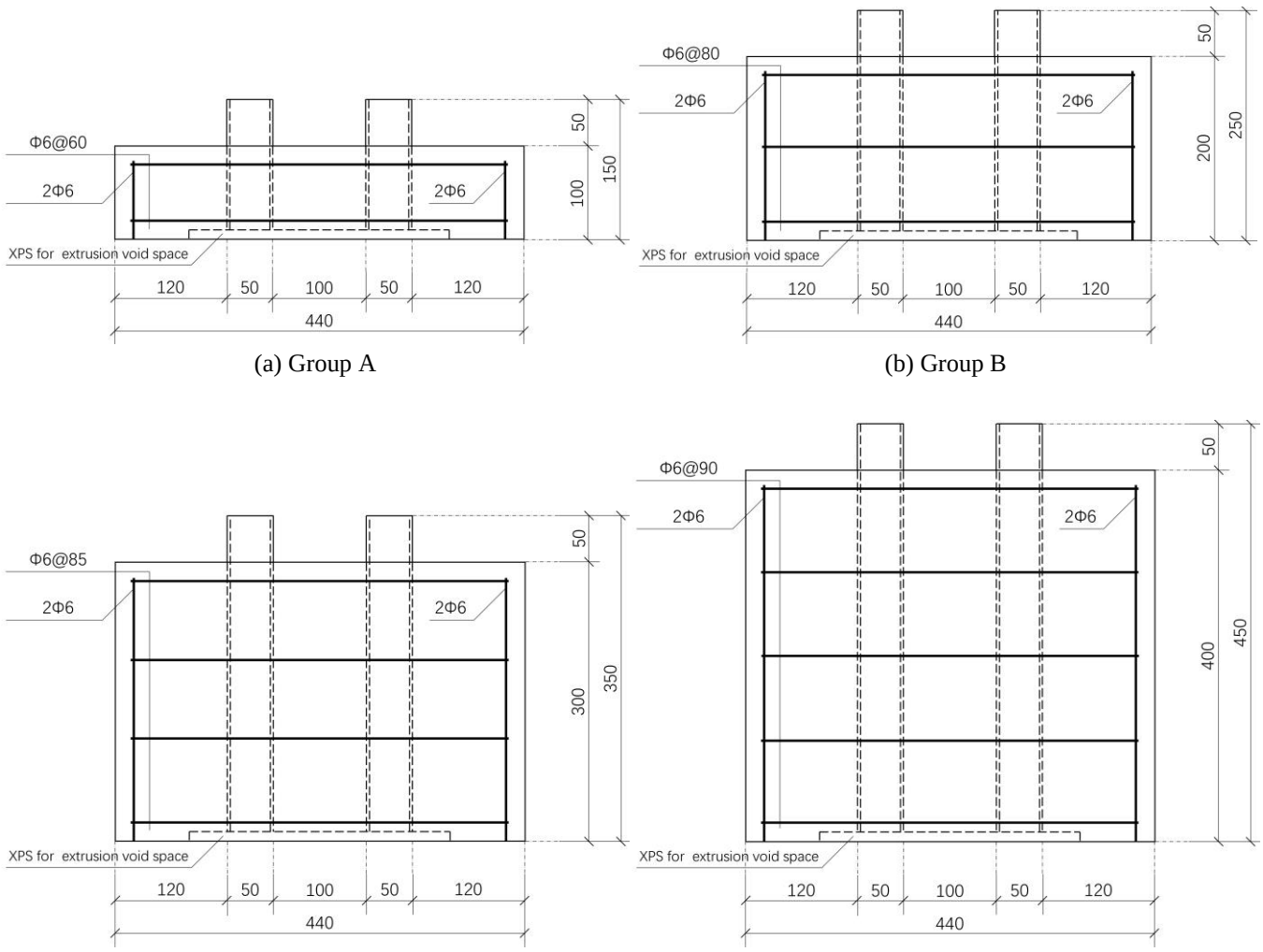

(a) Group A (b) Group B

(c) Group C (d) Group D

Figs. 2 Sections of Foam Concrete Specimens and C-Channels (XPS – extruded polystyrene to provide extrusion cavity, all dimensions in mm)

2.2 Test Specimen

2.2.1 Mix design of foam concrete

The foam concrete was casted with cement, sand, fly ash and foam. Cement and fly ash were mixed by using a high-speed electric mixer. Foam was added to the cement, and fly ash was added into the cement during the casting procedure. The slurry was poured into a steel mould with the reinforcing bars, stirrups, and C-Channels in place. All the samples have a fly ash/cement ratio of 25% and a water/cement ratio of 0.5. The water cement ratio was kept constant during the testing to provide a consistent strength of the foam concrete. However, the strength will change because of the density which is controlled by changing the volume of the foam. The composition of the materials in the foam concrete specimens is shown in Table 2.

Table 2 Composition of Foam Concrete

Density (kg/m^3)	Weight of Cement (kg/m^3)	Weight of Fly Ash (kg/m^3)	Weight of Water (kg/m^3)	Weight of Blowing Agent (kg/m^3)	Water/ Cement	Fly Ash/ Cement
800	456.36	114.09	228.18	1.37	0.50	0.25
1000	570.77	142.69	285.38	1.15	0.50	0.25
1200	685.18	171.29	342.59	0.94	0.50	0.25
1600	914.00	228.50	457.00	0.51	0.50	0.25

The foam concrete was initially cured in water for 24 hours and subsequently air cured in the mould for 7 days. After 7 days, the specimens were removed from the mould and cured for 28 days before testing. A plastic enclosure was used to surround the groups of concrete specimens to

keep the foam concrete from drying, thus reducing the possibility of shrinkage cracks.

2.2.2 C-Channels

The C-Channels are thin-walled C type cold formed steel with grade Q235. The C120 has a cross-sectional size of 120x 50x20 with a thickness of 3 mm. Vertical round bars with a diameter of ϕ 6 mm and made of Q235 grade steel were used for the transverse reinforcement. The C-Channels were prefabricated in factory and cold formed, and then manually cut and polished. The test specimens were made of steel with double sections; therefore, in the final stages of preparing the specimens, grinding was carried out to align the two channels to ensure that there was even loading on the flat and smooth contact surfaces on both channels. The round bars were modified, and cut, bent, bound and spot welded for the horizontal and vertical reinforcements.

3. Testing procedures

Prior to the testing, the C-Channels and foam concrete were visually examined for any obvious defects. To determine the mechanical characteristics of the C-Channel steel, specimens of the C-Channel steel and round re-bars were tested by following the current Chinese national standards found in *GB6397-86, 'Metal Tensile Test Specimens'* (National Standard of the People's Republic of China, 1986). The yield stress, ultimate tensile strength, elastic modulus, and Poisson's ratio are shown in Table 3. The yield stress of the cold formed steel is about 330 MPa with an ultimate tensile strength of 488 MPa. The elastic modulus is around 208 GPa with a Poisson's ratio of 0.26. The round re-bars have slightly lower mechanical parameters.

Table 3 Properties of Cold Formed Steel C-Channel and Re-bars

Specimen Type	Specimen No.	Yield Strength (MPa)	Ultimate Strength (MPa)	Elastic Modulus (GPa)	Poisson's Ratio	Elongation
Cold Formed Steel	1	330	488	208	0.26	0.27
	2	330	489	209	0.26	0.27
	3	329	487	209	0.26	0.27
	Average	330	488	208	0.26	0.27
	Std Dev	0.87	0.92	0.58		
Round bar	1	319	455	205	0.25	0.27
	2	317	452	205	0.25	0.27
	3	314	448	205	0.25	0.27
	Average	317	452	205	0.25	0.27
	Std Dev	2.49	3.91			

Testing was carried out at the Jilin Jianzhu University in Changchun, China, by using a YAW-2000kN hydraulic compression testing machine (as it shown in Figure 1 c). This hydraulic compression testing machine can be programmed by using a micro-control system which controls the load increment and records load-displacement measurements at the required intervals. The system can also detect the peak load and switch to a displacement control state to measure the post peak softening response. Since the strength of the foam concrete varied, depending on its density, load increments of 5, 10, 15 and 20kN were used on the specimens in Groups A, B, C, and D respectively. The rate of the application of the load was 0.2 kN/s until it reached the peak force. When the sample was loaded under displacement control, the loading rate was 0.01mm/s. The properties of the foam concrete of different densities are shown in Table 4.

Foam concrete blocks with a C-Channel were tested under compression. Each test was repeated three times to account for small variations in the test results. The average value of each test is reported as follows.

Table 4 Properties of Foam Concrete

Test Block No.	Density (kg/m^3)	Failure Loading (kN)	Compressive Strength (MPa)	Average Compressive Strength (MPa) (Std Dev)	Average Failure Loading (kN)
800-1	813	224	10		
800-2	807	210	9.3	9.62	1.18
800-3	808	216	9.6	(0.32)	
1000-1	1003	297	13.2		
1000-2	1006	304	13.5	13.57	1.48
1000-3	1007	316	14	(0.42)	
1200-1	1211	463	18.3		
1200-2	1209	448	17.9	18.08	1.79
1200-3	1206	481	18.1	(0.18)	
1600-1	1604	552	24.5		
1600-2	1598	518	23	23.68	2.14
1600-3	1596	528	23.5	(0.78)	

4. Tests Results

Group A specimens have the smallest depth of 100 mm and therefore the least amount of surface area in the concrete bonding with the steel. The vertical force versus vertical displacement plots are shown in Figure 3A. With different densities, the maximum measured vertical forces are 31, 35, 41, and 53 kN for foam concrete densities of 800, 1000, 1200 and 1600 kg/m^3 respectively. All the specimens

show a peak force followed by a steady decline of the vertical force to a residual value that varies from 12 to 23 kN. The residual values are reached at a vertical displacement between 3 to 4 mm. The tests were terminated at 6 mm. It was observed that all the specimens reach the peak stress at a vertical displacement of about 0.7 mm, regardless of the density of the foam concrete.

Similar test results were obtained for the specimens in Groups B, C, and D as shown in Figures 3B, 3C, and 3D respectively. It is noted that the specimens in Groups B, C, and D have concrete embedment depths of 200, 300 and 400 mm respectively. The results show remarkable similarity with the peak force measured at a vertical displacement of approximately 0.7 mm. In all cases, there is a steady decline from the peak to residual force and the residual force is reached at a displacement between 3 and 4 mm. Of course, the peak and residual forces increase with higher density and increased specimen thickness.

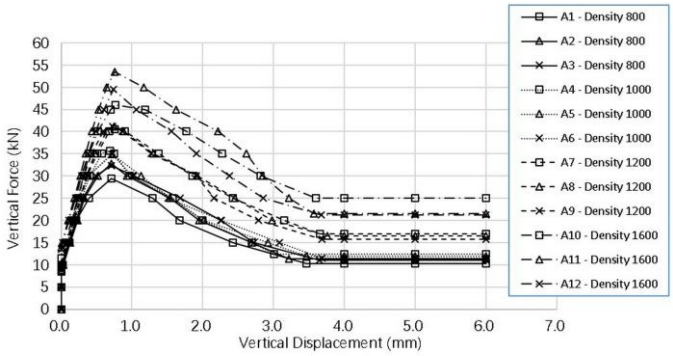

(a) Force Displacement Plot of Group A Specimens

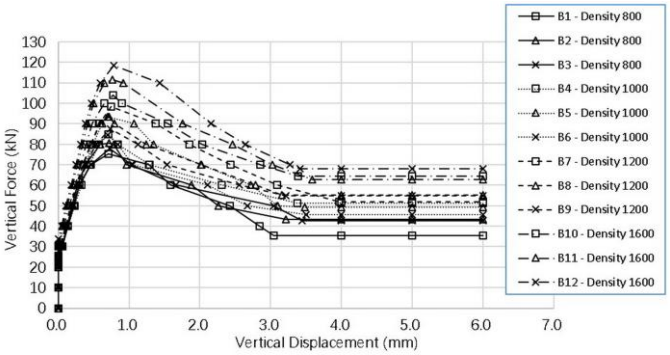

(b) Force Displacement Plot of Group B Specimens

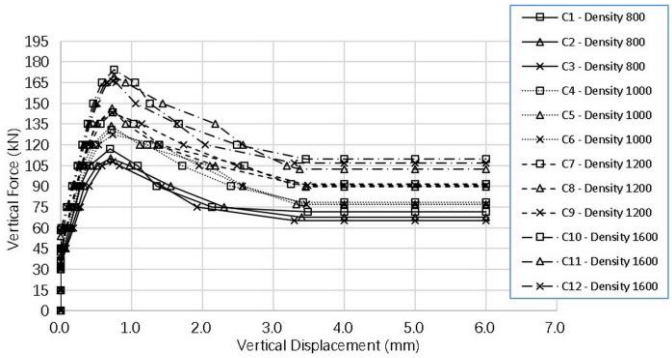

(c) Force Displacement Plot of Group C Specimens

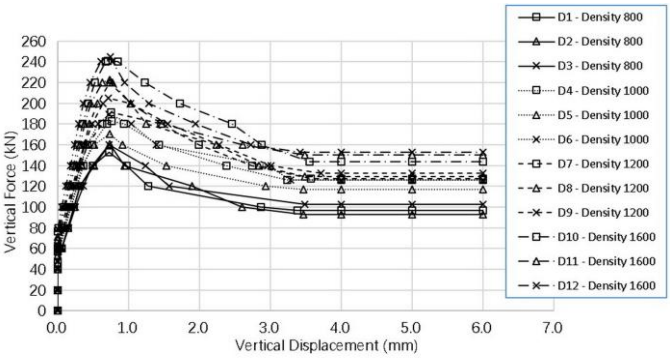

(d) Force Displacement Plot of Group D Specimens

Figs.3 Force Displacement Plot of All Specimens

4.1 Tests Results with Different Densities

The vertical force-displacement plots for the different specimen groups and densities are provided in Figure 3 for densities of 800, 1000, 1200, and 1600 kg/m^3 respectively. It can be seen in the figure that the peak vertical force increases when the depth of the specimen increases.

However, the peak vertical displacements are approximately the same at a value of 0.7 mm. The graphs are remarkably similar for density variations of800 to 1600 kg/m^3. This suggests a very similar failure mechanism in all these cases except for the increase in the strength of the foam concrete.

4.2 Force and Displacement Behaviour

After statistically analysis of the data, the information was then plotted onto a curve (see Figure 4).

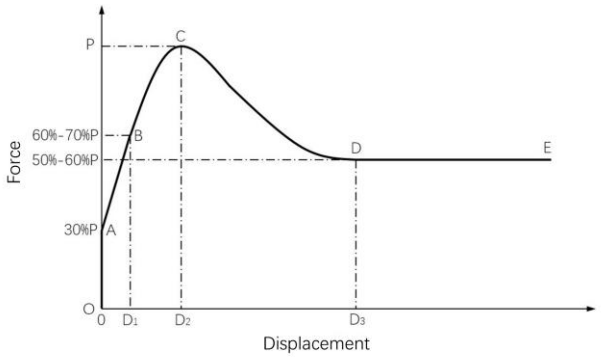

Fig. 4 Force and Displacement Behaviour Curve

The C-Channel remained elastic and its surface was smooth. Therefore, it can be concluded in this work that there is no interlocking mechanism between the cold

formed steel and foam concrete. Thus, the different bonding forces found during the loading process of the samples show that the curve can be analytically interpreted as follows:

1. Area of vertical increase (OA segment). During the early periods of load testing, before the vertical force reached about 30% of the peak force, the amount of displacement of the end load did not show any significant changes. There were only slight changes in the pressure generated by the C-Channels during compression. During this process, the applied load was supported by the chemical bonding force. Both types of materials worked well with each other.
2. Area of linear increase (AB segment). The chemical bonds began to break down during this stage, and a relative amount of slippage started between the C-Channels and foam concrete. In the process, the chemical bonding was still adequately strong enough, which meant that the adhesion resistance countered the imposed loading caused by the generated frictional resistance. As well, an increasing linear relationship can be observed.
3. Upward slope of curve (BC segment). Even though the chemical bonding is similar to that found in the AB segment after the loading reached about 60%-70% of the peak force, the chemical bonding force did almost not exist and the frictional resistance increased nearly to the limit. Thus, the magnitude of the displacement is substantially increased accompanied with faint sounds of splitting.
4. Area of decline (CD segment). There was no chemical bonding when the load reached the peak force. Only the remaining frictional resistance bore the load. At that time, the strain of the C Channels was substantially reduced and the normal pressure on the foam concrete was reduced, thus leading to a reduction in the frictional resistance. The splitting sound continued, and each specimen exhibited the greatest difference in the area of decline. The local linear line, curve, and broken lines have a descending trend.
5. Horizontal section (DE segment). After the vertical force was reduced to about 50%-60% of the peak force, the sound of splitting stopped, and the frictional resistance no longer decreased. Thus, the residual force stabilized.

4.3 Variation of Peak Forces

To examine the effect of density and specimen thickness on the measured peak force, the peak force versus concrete density was plotted for the different groups, see Figure 5. It can be seen that as the density of the foam concrete increases, the peak forces also increase. However, the curves for the different groups of specimens, A, B, C, and D are more or less parallel to each other when the densities increase from 1000 to 1600 kg/m^3. The lines of the lower densities, 800 to 1000 kg/m^3, have different slopes than those of the higher densities and the slopes change to become steeper when the specimen thickness is increased from 100 to 400 mm.

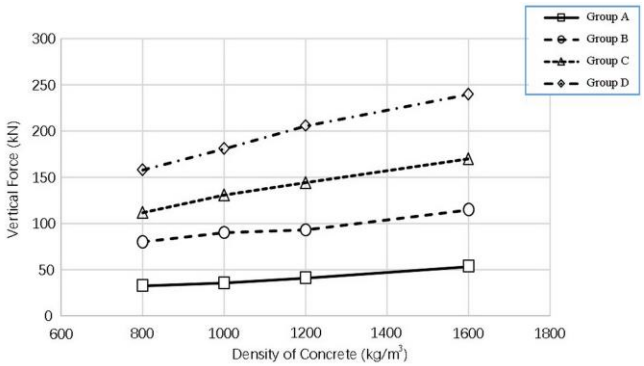

Fig. 5 Peak Force versus Foam Concrete Density

Figure 6 shows the changes in the peak vertical force versus the different groups of specimens (or different concrete thicknesses). It is obvious that as the specimen thickness increased, the peak vertical force also increases. However, the increase in vertical force is much greater for higher strength concrete than lower strength concrete, which could be due to the changes in the mechanism of failure. When the strength of the concrete is increased, the shear stresses can be transferred to a larger volume of material which leads to an additional increase in shearing resistance.

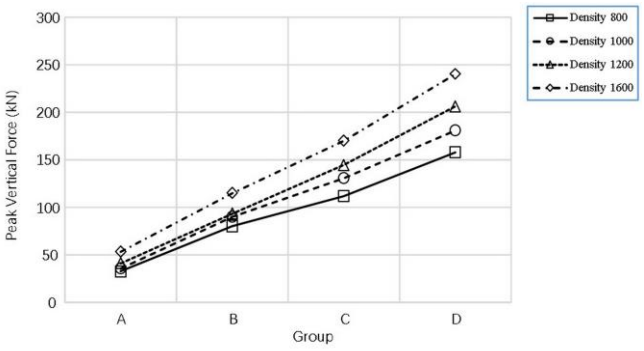

Fig. 6 Peak Force for Different Groups of Specimens

4.4 Modes of Failure

The observed failure modes for the Group A specimens are shown in Figure 7. Figure 7shows the top and bottom views of the specimens after failure and the changes in the failure pattern for foam concrete densities from 800 to 1600 kg/m^3. It can be seen from the bottom view of the specimens that the failure mode for a lower density of concrete of 800 kg/m^3 is shearing along the interface between the steel channel and the concrete. There is minimum failure away from the channel perimeter. As the density of the concrete increases, which means that as the strength of the concrete is increased, more extensive failure is observed away from the C-Channel. Ironically, higher shear strength of concrete results in more extensive failure. This is due to the ability of the material to transfer the shear stress away from the C-Channel.

(a) Top view of sample with density 800

(b) Bottom view of sample with density 800

(c) Top view of sample with density 1000

(d) Bottom view of sample with density 1000

(e) Top view of sample with density 1200

(f) Bottom view of sample with density 1200

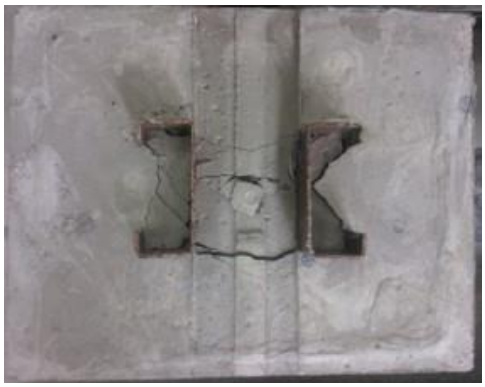

(g) Top view of sample with density 1600

(h) Bottom view of sample with density 1600

Figs. 7 Failure Modes of Group A Specimens (A, C, E, and G are top surface and B, D, F, and H are bottom surface for foam concrete densities of 800, 1000, 1200 and 1600 kg/m3, respectively)

The failure modes for specimens in Groups B, C, and D during testing were similar. The top surface and sides remained intact. Only minor cracks appeared on the bottom surface. Specimens with greater depths of concrete thickness had lower degrees of cracking. From the "core area" A (the core is defined as the material confined inside each C-Channel in the specimen, and the core area is the bottom area of the core) on the bottom surface of the specimens, the failure modes appeared to be similar to those of Group A, but when a hammer was used to crack the specimens, it was found that there are fundamental differences in the specimens in Group A. These include slippage of a thin layer of the foam concrete because the relative concentration of the stress at the bottom had led to splitting, while the inside of the foam concrete remained intact. Shear(bond) failure therefore takes place in these specimens. The failure modes of the specimens are shown in Figure 8. It is seen from the actual failure mode observed in the experiment that failure is confined to the centre "core" region enclosed by the C-Channels. This is called Mode 1A failure.

(a) Top view of Group B Sample

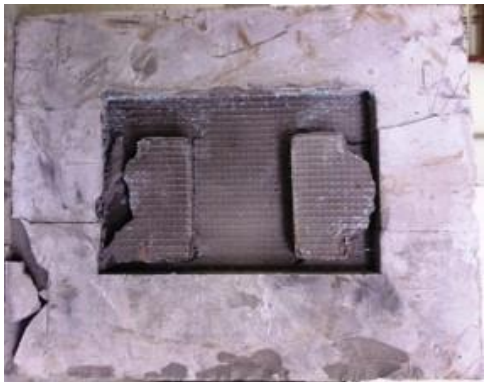

(b) Bottom view of Group B Sample

(c) Top view of Group C Sample

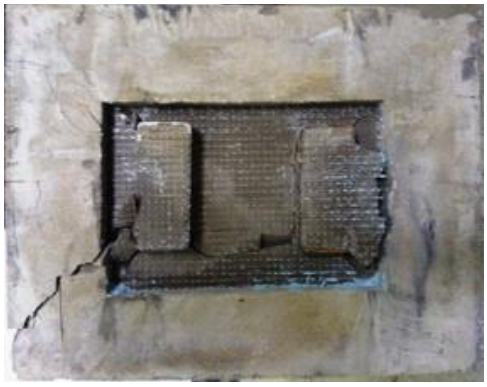

(d) Bottom view of Group C Sample

(e) Top view of Group D Sample

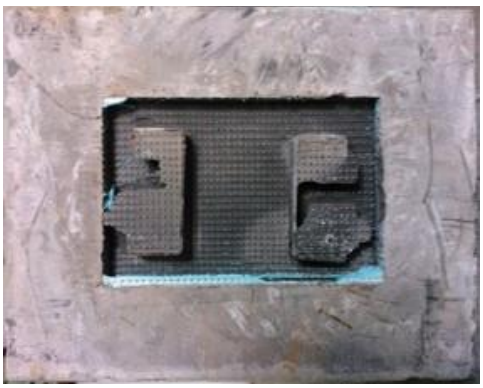

(f) Bottom view of Group D Sample

Figs. 8 Failure Modes of Group Specimens (A, C, and E are top surface and B, D, and F are bottom view of Groups B, C, and D respectively).

The damage in the specimens in Group A are worth noting: shear(bond) failure took place in the initial stages of loading. However, when the load was between 70% and 80% of the maximum load, splitting failure occurred in the core areas of the foam concrete and the sound of splitting could be heard. Afterwards, the splitting sounds

continued, but stopped upon reaching the section with the residual bond stress. When the loading was completed, it was observed that the foam concrete samples were intact and had not split, see Figure 7for the specific failure modes of the samples in Group A. Figure 9 summarized the modes of failure. Four modes of failure can be identified.

1. Mode of failure 1 and 1A

Bond failure at the interface between the steel and foam concrete around the perimeter of the C-Channel, that is, both the inside and outside perimeters. The failure involves the core material inside the C-Channel. Mode 1A involves failure at the interface between the steel and foam concrete on the outside perimeter, but not on the inside perimeter of the C-Channel. In developing a mechanism of failure in Mode 1A, failure occurs in the foam concrete between the steel flanges.

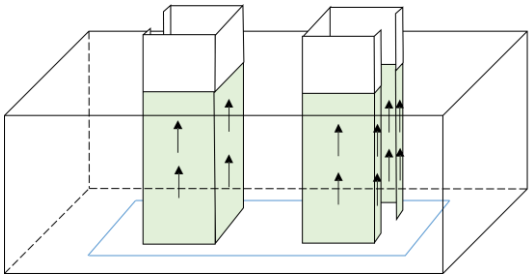

(a) Mode 1 – Shearing at steel concrete contact including inside C channel

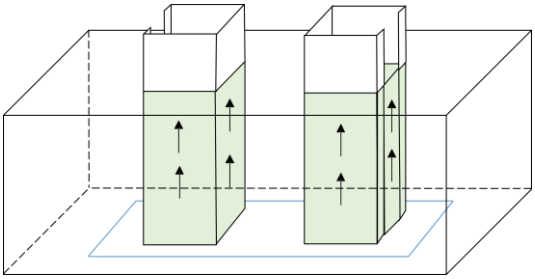

(b) Mode 1A – Shearing at steel concrete contact and concrete inside C channel fails as a block

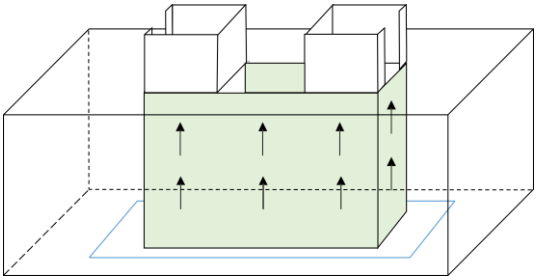

(c) Mode 2 – Shearing of two channels together

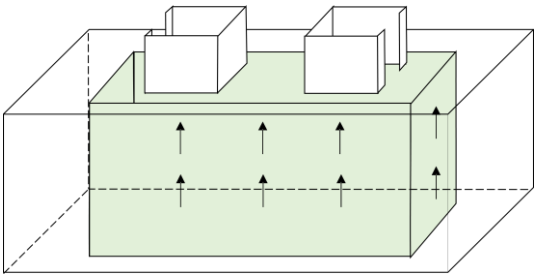

(d) Mode 3 – Shearing of extrusion block

Figs. 9 Modes of Failure

2. Mode 2 failure of the two C-Channels together
3. Mode 3 concrete block extrusion

Based on the experimental observations, Modes 2 and 3 have not been observed for the range of densities and strengths of the foam concrete that were tested. Both Modes 2 and 3 provide much higher resistances compared to Modes 1 and 1A since they involve much larger surface areas of concrete failure.

Previous studies have found that the failure of brittle concrete is mainly attributed to the splitting of the whole concrete (Min et al. 2014, Bažant and Cedolin 2003, Stratford and Burgoyne 2003), but rarely in cases where the core area is split as found from the failure modes of the specimens in this study. The reasons could be as follows: The C section steel has greater lateral restraint, which influences the stress state of the concrete in the core areas, due to the characteristics of the cross section and lack of thickness of the cold formed thin walled C section steel samples. On the other hand, foam concrete has lower strength because it does not contain coarse aggregates, and therefore it has lower shear strength than ordinary concrete. Consequently, when there is sufficient lateral restraint, the foam concrete that is outside the core area will not incur severe damage.

The embedment length of the specimens in Group A was shorter in comparison to those in Groups B, C, and D. Therefore, the inferred embedment length is too short, thus leading to failure due to splitting in the core areas of the foam concrete. In comparing against the density of the specimens in Group A, it was found that splitting occurs in the core areas of the samples with a density of 800 and 1000 kg/m^3. However, it was also found that splitting occurs in the core areas of the specimens with a density of 1200 and 1600 kg/m^3 in both Groups A and B. Therefore, it can be inferred that as the strength of the foam concrete increases, the brittleness also increases, in that the cracking damage on the bottom surface is more pronounced.

5. Calculation of Peak force for Different Modes of Failure

The method to calculate the peak force for all 4 modes is developed here, it was assumed that the mobilized shear stress was uniformly distributed along the failure surfaces.

Peak Force Calculation

The peak force for Mode 1 can be calculated from:

$$P = 2\,\alpha\,\tau_\phi\,A_c\,d \qquad (1)$$

where P is the peak vertical force; $\alpha$is the steel-concrete interface coefficient; τ_ϕ the shear strength of the foam concrete; A_c is the circumferential area of contact between the steel and concrete; and d is the depth of the steel C-Channel in the concrete block. The peak force for each channel is multiplied by 2 for two channels.

For Mode 1, A_c is calculated based on two sides, the inside and outside surface areas of the C-Channel. If α = 1, failure is assumed to occur in the concrete. For Mode 1A, A_c can be determined based on the outside perimeter of the C-Channel and the concrete between the steel flanges, see Figure 9. For Modes 2 and 3, A_c is based on the perimeter of the failure block between the C-Channels or the extrusion block respectively.

The maximum vertical force can be calculated for different modes of failure based on the shear strength of the foam concrete to be about 8% of the compressive strength as shown in Table 4. The ratio is based on information provided by the Pan Pacific Management Resources Pty. Ltd. (2015). Also based on previous work on the slippage between steel and foam concrete, an αvalue was used in the calculation, see Ikponmwosa et al. (2014). The results are shown in Table 5. In table 5, the coefficient α is determined through the longitudinal shear failure between the steel-concrete interface, if α= 1, the failure is assumed to occur in the concrete, the value of α in other failure mode can be therefore worked out correspondently the measured peak forces are shown in Table 6. For a comparison between the calculated and measured peak forces, their values are plotted in Figure10. Figure10 shows the comparisons between the measured and calculated peak vertical forces. The legend of Figure 10 identifies different modes of failure in the calculation. In the legend, A-1AC denotes that the calculation is based on Mode 1A (A-**1A**C), assuming failure through the concrete (A-1A**C**) for Group A (**A**-1AC) specimens, and A-1AS denotes the same except that failure occurs at the steel and concrete interface. In other words, the strength of the concrete is used in the calculation of the peak force for the failure in Mode 1 in A-1AC and the interface strength is used in the calculation of the peak force for the failure in Mode 1 in A-1AS. The test result from Figure 10 shows that, a stronger bonding between the concrete and the steel C channel embedment was observed compare to the theoretical calculation, the reason behind that is, when the crack is developed in the foam concrete, the anchorage force between the two interfaces are increased in a certain extent due to the dowel action between the concrete and the embedment. Therefore, higher bond values are observed from the tests.

Table 5 Calculated Peak Compressive Force on C-Channels

Mode	Concrete Density (kg/m^3)	Shear Strength of Concrete (kPa)	α	Peak Vertical Force (kN) Group			
				A	B	C	D
1C	800	750	1	78	156	234	312
	1000	850	1	88	177	265	354
	1200	950	1	99	198	296	395
	1600	1200	1	125	250	374	499
1S	800	750	0.7	55	109	164	218
	1000	850	0.7	62	124	186	248
	1200	950	0.7	69	138	207	277
	1600	1200	0.7	87	175	262	349
1AC	800	750	1	51	102	153	204
	1000	850	1	58	116	173	231
	1200	950	1	65	129	194	258
	1600	1200	1	82	163	245	326
1AS	800	750	0.7	39	79	118	157
	1000	850	0.7	45	89	134	178
	1200	950	0.7	50	100	149	199
	1600	1200	0.7	63	126	189	252
2	800	750	1	90	180	270	360
	1000	850	1	102	204	306	408
	1200	950	1	114	228	342	456
	1600	1200	1	144	288	432	576
3	800	750	1	138	276	414	552
	1000	850	1	156	313	469	626
	1200	950	1	175	350	524	699
	1600	1200	1	221	442	662	883

Table 6 Measured Peak Vertical Force on C Channel

Concrete Density (kg/m^3)	Shear Strength of Concrete (kPa)	Peak Vertical Force (kN) Group			
		A	B	C	D
800	750	31	78	112	158
1000	850	35	88	131	181
1200	950	41	93	144	206
1600	1200	50	111	170	236

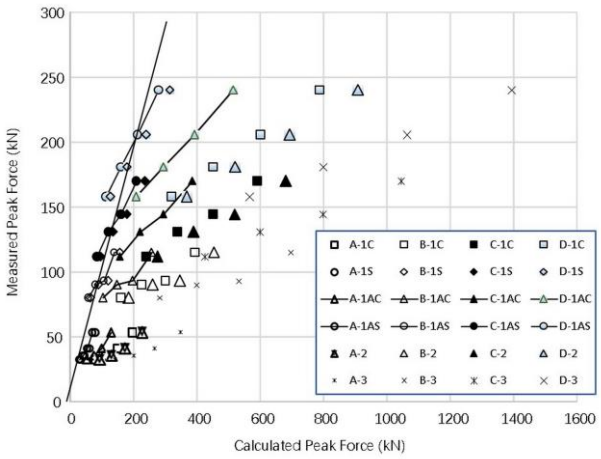

Fig. 10 Comparison between Measured and Calculated Peak Vertical Forces for Different Modes of Failure. (First letter in the legend denotes the group and the number denotes the failure mode. Mode 1AC refers to Mode 1A assuming failure occurs in concrete only. There is no slip failure between the concrete and the steel. Model 1AS refers to failure in the concrete and at the interface between steel and foam concrete when steel is present.)

A line which shows the equal values of the calculated and observed data is drawn on each graph for comparison purposes. Point on or close to the lines represent a good match between the calculated and observed data. It is obvious that the calculations of Modes 2 and 3 have over-predicted the peak vertical forces since they assume a much larger failure zone than observed. It is seen that Mode 1A provides the best agreement between the measured and calculated peak vertical forces. This is consistent with the experimental observations of the failure mode in which failure is confined close to the C-Channel. The α coefficient in this case has a value of 0.4 based on a calibration of the test results, thus indicating weak bonding between the concrete and the steel. This coefficient was determined based on the measurement of the applied loads in this case. Although the coefficient was calibrated against the experimental results, only one coefficient was used for all the analyses which justify the use of Equation (1) and the assumed mode of failure. The mode of failure in this case involves the foam concrete inside the C-Channel becoming part of the channel during failure.

6. Result Discussion

The failure of the cold formed steel C-Channel sand foam concrete shows a longitudinal shear failure mode that involves slipping between the interface of the steel and concrete as well as through the foam concrete. The foam concrete inside the C-Channels forms part of the failure mass under the maximum stress. For low density foam concrete, which means lower shear strength, the failure involves a narrow region close to the steel. When the strength of the concrete is increase, shear failure propagation results in a larger shearing region in the foam concrete. This however did not result in a much larger failure zone that involved both channels failing as an entity. This is observed in both the experiments as well as the theoretical analysis.

An interesting experimental observation is that the vertical displacement at the peak force was measured to be approximately 0.7 mm and independent of the strength of the foam concrete and specimen thickness. This means that the slipping along the steel-concrete interface is uniform due to the much higher stiffness of the steel channel as opposed to that of the foam concrete. If the steel channel compresses non-uniformly or progressively when the vertical force is increased due to shear development along the channel, the displacement at the peak force will increase when the depth of the specimen increases. This is evident in the results reported by Ramezani et al. (2013) who show an increase in the peak force displacement when the bonding between the steel and concrete increases. Although the tests carried out in Ramezani et al. (2013) were conducted in tension, the mechanism on the effect of the peak-force displacement is the same. In addition, if the bond-slip displacement increases with increases in the strength of the foam concrete, the displacement at the peak force will also increase when the strength of the concrete is increased. This is another confirmation of the Mode 1A failure mode since concrete stiffness and strength increase with increases in density but the stiffness of the interface resistance will not increase.

It is observed that the measured maximum vertical force shows a linear relationship with the thickness of the specimens in Groups A to D. However, as the density of the foam concrete increases, the specimen thickness has more effects on the measured peak force. That is, the constant density lines are not parallel to each other. On the other hand, the measured maximum vertical force is found to have a bi-linear relationship with the density of the concrete. The slight change in the slope of the line is an indication of the increase in the failure region around the steel channel with increased density.

The proposed model provides a framework for analysing the shear bonding strength of foam concrete with cold-formed steel C-Channels. It is obvious that the maximum shear bonding strength not only depends on the density of the foam concrete, but also on the loading rate, confinement, and the amounts of stirrups. The proposed framework is applicable to the configuration tested in this work.

7. Conclusions

Based on the experimental tests and theoretical analysis, the following conclusions can be made:

- The failure mechanism of the double C-Channels involves shear failure at the interface between the steel and concrete and shearing portion of the concrete inside the channels.
- Based on the measured strength of the foam concrete, the failure mode that mostly matches the measured peak forces is Mode1A on the failure at the steel-concrete interface and through the concrete. This also agrees with the experimental findings based on observations of the bottom of the specimens.
- It is also found that the force-displacement shows a peak value followed by a gradual decline to a residual force. The peak force is dependent on the strength of the foam concrete as well as the thickness of the specimens. The displacement at the peak force is independent of the density/strength of the concrete and the specimen thickness. This is further confirmation of Mode 1A failure mode. The peak load is bi-linearly related to the density of the foam concrete and linearly related to the thickness of the specimen.
- End slip is uniformly mobilized along the C-Channels which is evidenced by a peak vertical displacement independent of the strength of the foam concrete and embedment depth of the steel.

Acknowledgement

The authors gratefully acknowledge funding from the National Natural Science Foundation of China.

Project name: Failure mechanism research for lightweight steel and foam concrete composite structure

Approval number: 51378238

Notation

The following symbols are used in this paper:

A_c= circumferential area of contact between steel and concrete

φ = diameter of stirrup

τ_ϕ = shear strength of the foam concrete

α = steel-concrete interface coefficient

References

Bažant, Z.P. and Cedolin, L. (2003). *Stability of Structures: Elastic, Inelastic, Fracture, and Damage Theories*, Oxford, Dover Publications, New York.

Flores-Johnson, E.A. and Li, Q.M. (2012). "Structural behaviour of composite sandwich panels with plain and fibre-reinforced foamed and corrugated steel faces." *Composite Structures*, **94**(5), 1555-1563.

National Standard of the People's Republic of China (1986). *Metal Tensile Test Specimens*. GB6397-86. China.

Heath D, Gad E. *Design Guidelines for Cast-In and Post-Installed Anchors in Australia*, ASCE 2014.

Hilal, A.A., Thom, N.H. and Dawson, A.R. (2015). "The use of additives to enhance properties of pre-formed foamed concrete." *International Journal of Engineering and Technology*,**7**(4), 286-293.

Ikponmwosa, E., Falade, F., Fapohunda, C, Akinniyi, T. and Olori, K. (2014). "Effect of foam concentration on structural characteristics of steel reinforced aerated concrete beams." *Pacific Journal of Science and Technology*, **15**(1), 32-46.

Lim, S., Tan, C., Zhao, X., and Ling, T. (2014). "Strength and toughness of lightweight foamed concrete with different sand grading." *KSCE Journal of Civil Engineering*, 10.1007/s12205-014-0097-y.

Min, F., Yao, Z. and Jiang, T. (2014). "Experimental and numerical study on tensile strength of concrete under different strain rates." *Scientific World Journal*, 2014.

Mydin, M.A.O., Wang, Y.C. (2011). "Elevated-temperature thermal properties of lightweight foamed concrete." *J. Construction and Building Materials*, **25**, 705-716.

Nambiar, E.K. and Ramamurthy, K. (2008). "Fresh state characteristics of foam concrete." *J. Mater. Civ. Eng.*, 10.1061/(ASCE)0899-1561(2008)20:2(111).

Othuman, M.A. and Wang, Y.C. (2011). "Elevated-temperature thermal properties of lightweight foamed concrete." *J. Construction and Building Materials*, **25**, 705-716.

Mohamad, N., Khalil, A.I., Abdul Samad, A.A. and Goh, W.I. (2014). "Structural behavior of precast lightweight foam concrete sandwich panel with double shear truss connectors under flexural load." *ISRN Civil Engineering*, 2014.

Pan Pacific Management Resources Pty. Ltd. (2015). "Lightweight, foamed or cellular concrete technology." <http://www.litebuilt.com> (May 15, 2015).

Ramezani, M., Vilches, J., and Neitzert, T. (2013). "Pull-out behavior of galvanized steel strip in foam concrete." *International Journal of Advanced Structural Engineering*, **5**(24).

Stratford, T. and Burgoyne, C. (2003). "Shear analysis of concrete with brittle reinforcement." *J. Compos. Constr.*,10.1061/(ASCE)1090-0268(2003)7:4(323).

Tan, C.S., Lee, Y.L., Mohammad, S., Lim, S.K., and Lee, Y.H. (2015). "Interaction between cold-formed steel and lightweight foamed concrete with various cement content." *Malaysian Journal of Civil Engineering*, **27**(1), 115-127.

Thakrele, M.H. (2014). "Experimental study on foam concrete." *International Journal of Civil, Structural, Environmental and Infrastructure Engineering Research and Development*, **4**(1) 145–158.

Wan Ibrahim, M.H., Jamaluddin, N., Irwan, J.M., Ramadhansyah, P.J. and Suraya Hani, A. (2014). "Compressive and flexural strength of foamed concrete containing polyolefin fibers." *Advanced Materials Research*, **911**, 489-493.

Warren G. E., "Anchorage strength of tensile steel in reinforced concrete beams", Ph.D. Dissertation, Iowa state University.1969.

Yue, L. and Bing, C. (2015). "New type of super-lightweight magnesium phosphate cement foamed concrete." *Journal of Materials in Civil Engineering*, 10.1061/(ASCE)MT.1943-5533.0001044, 04014112.